Development 128, 4873-4880 (2001)
Printed in Great Britain © The Company of Biologists Limited 2001
DEV2809

Fgf/MAPK signalling is a crucial positional cue in somite boundary formation

Atsushi Sawada[1,2], Minori Shinya[1,2], Yun-Jin Jiang[3], Atsushi Kawakami[1], Atsushi Kuroiwa[2] and Hiroyuki Takeda[1,*,‡]

[1]Division of Early Embryogenesis, National Institute of Genetics, Mishima, 411-8540 Japan
[2]Division of Biological Science, Graduate School of Science, Nagoya University, Nagoya 464-8602, Japan
[3]Vertebrate Development Laboratory, Imperial Cancer Research Fund, 44 Lincoln's Inn Fields, London WC2A 3PX, UK
*Present address: Department of Biological Sciences, Graduate School of Science, The University of Tokyo. Hongo, Bunkyo-ku, Tokyo, 113-0033, Japan
‡Author for correspondence (e-mail: htakeda@biol.s.u-tokyo.ac.jp)

Accepted 29 August 2001

SUMMARY

The temporal and spatial regulation of somitogenesis requires a molecular oscillator, the segmentation clock. Through Notch signalling, the oscillation in cells is coordinated and translated into a cyclic wave of expression of *hairy*-related and other genes. The wave sweeps caudorostrally through the presomitic mesoderm (PSM) and finally arrests at the future segmentation point in the anterior PSM. By experimental manipulation and analyses in zebrafish somitogenesis mutants, we have found a novel component involved in this process. We report that the level of Fgf/MAPK activation (highest in the posterior PSM) serves as a positional cue within the PSM that regulates progression of the cyclic wave and thereby governs the positions of somite boundary formation.

Key words: Fgf, Somite, Segmentation, Tailbud, *fused somites*, *after eight*, *her1*, Zebrafish

INTRODUCTION

Somite formation, a process in which reiterated epithelial structures are progressively demarcated from the mesenchymal presomitic mesoderm (PSM) in a rostrocaudal sequence, is the earliest manifestation of segmentation and is a feature shared by all vertebrate embryos. The strict temporal and spatial regulation of somitogenesis is of crucial importance because it governs the metamerism of all somite-derived tissues: axial skeleton, the dermis of the back and all striated muscle of the adult body, and spinal ganglia.

The understanding of the molecular mechanisms creating periodicity of somite formation has been greatly advanced in the last few years. The remarkably cyclic expression pattern of chick *hairy1*, a *hairy*-related bHLH transcription factor, in the PSM provided the first evidence for an intrinsic molecular clock linked to somitogenesis (Palmeirim et al., 1997). The presence of the clock in vertebrate PSM was further supported by the periodic expression of several genes including other *hairy*-related genes in mouse (Jouve et al., 2000) and zebrafish (Sawada et al., 2000; Holley et al., 2000), and genes implicated in the Notch signalling pathway, *lunatic fringe* in mouse (Aulehla and Johnson, 1999; Forsberg et al., 1998) and chick (McGrew et al., 1998) or *deltaC* and *deltaD* in zebrafish (Jiang et al., 1998). The expression stripes of these genes appear in the tailbud each somite cycle, sweep caudorostrally across the PSM, and finally stabilize in the anterior PSM before segment border formation. Recent genetic studies in mouse and zebrafish demonstrated that Notch/Delta signalling is required for synclonization of the segmentation clock in the PSM (Jiang et al., 1998; Jiang et al., 2000; Pourquié, 1999).

Existence of the clock in the PSM has been predicted by theoretical models such as 'clock and wavefront' (Cooke and Zeeman, 1976; Dale and Pourquié, 2000). In this model, the clock creates a temporal periodicity, such as a cyclic wave of gene expression, which would later be interpreted by the wavefront to generate spatial periodicity of the somites. The wavefront that exists in the anterior PSM gradually moves back as somitogenesis proceeds. Thus, the stepwise interaction between the clock and the wavefront (or periodic entry of the wave into the wavefront) leads to regularly spaced furrow formation. The model also predicts the presence of positional information restricting the wavefront to the anterior PSM. In facts, PSM cells, born in an immature state in the tailbud, become matured as they pass the intermediate to the anterior PSM, and finally acquire the wavefront activity that arrests the cyclic gene expression and initiates somite furrow formation (Holley et al., 2000). The zebrafish *fused somites* (*fss*) mutation bocks this maturation process, leading to no segmentation in the paraxial mesoderm (Holley et al., 2000; van Eeden et al., 1998). Although accumulated data of vertebrate somitogenesis support the 'clock-and-wavefront' model, the presence and molecular nature of the positional information within the PSM are totally unknown.

Fgf receptor (Fgfr)-mediated signalling is implicated in somitogenesis: *Fgfr1* is expressed in the PSM and the anterior part of segmented somites in mice and zebrafish (Sawada et al., 2000; Yamaguchi et al., 1992) and *Fgfr1* knockout mice produce embryos with disturbed segment borders (Yamaguchi

et al., 1994). Mice and zebrafish *fgf*8 mutants, however, do not proceed through gastrulation and do not show severe somitogenesis phenotypes, respectively (Sun et al., 1999; Reifers et al., 1998). Thus, in part due to early vital function and/or genetic redundancy of Fgf family and receptor genes, the precise role of Fgf signalling in segmentation has remained unclear. We report that Fgf/mitogen-activated protein kinase (MAPK) signalling activated in the posterior PSM is a crucial positional cue in restricting the maturation wavefront in the anterior PSM and maintains posterior PSM cells in an immature state in an *after eight/deltaD*- and *fss*-independent manner.

MATERIALS AND METHODS

Fish embryos

Zebrafish, *Danio rerio*, were maintained at about 26°C on a 14 hour light/10 hour dark cycle. Embryos obtained from natural crosses were staged according to Kimmel et al. (Kimmel et al., 1995). The mutants used were *fused somites* (*fss*^{ti1}) and *after eight* (*aei*^{tr233}).

Whole-mount in situ hybridization

Whole-mount in situ hybridization was performed as described in Nikaido et al. (Nikaido et al., 1997).

Immunohistochemistry and western blot

For whole-mount immunostaining, embryos were fixed with 3.7% formaldehyde/0.2% glutaraldehyde/phosphate-buffered saline (PBS) for 1 hour at the room temperature. After washing with PBS, they were dehydrated with methanol and transferred to PBS. They were washed with MABT (Maleic buffer (0.15 M maleic acid, 0.1 M NaCl pH. 7.5 (MAB)/0.1% Triton X-100)) three times for 10 minutes, and MABDT (MAB/0.1% Triton X-100/1% DMSO) twice for 30 minutes. After blocking with 2% FCS/MABDT, the embryos were incubated in the blocking solution containing 1:10000 anti-di-phosphorylated ERK1 abd ERK2 (MAPK-YT) antibody (Sigma) at 4°C overnight. They were then washed with MABDT three times for 5 minutes, four times for 30 minutes, and incubated in blocking solution again for 30 minutes, followed by incubation with the second antibody (1:500 anti-mouse IgG biotin conjugated antibody) for 2 hours at the room temperature. After the washing with MABDT as described above, the signals were detected with ABC staining kit according to the manufacturer's instruction (Vector Laboratory). For labelling mitotic cells, 1:200 dilution of anti-phosphorylated histone H3 (Upstate Biotechnology) was used as the first antibody (Saka and Smith, 2001).

Western blot analysis was performed following of the standard method for ECL western Blotting Detection Reagent (Amersham Pharmacia Biotech). Protein (10 μg/lane) were separated by 12.5% polyacrylamide gels and transferred to Hybond^{TM} ECL^{TM} membranes (Amersham Pharmacia Biotech) by electroblotting. Monoclonal antibody against dpERK was used at the same concentration as used for immunostaining. Yolk cell was removed from embryos before homogenization. The results were analysed by use of Limi-Imager and Lumi Analyst (Roche Molecular Biochemicals).

Beads transplantation and SU5402 treatment

Heparin-insolubilized acrylic beads (Sigma) were washed three times in PBS and soaked in 0.5 μg/μl mouse recombinant FGF8b protein (R&D Systems) or 0.5 μg/μl BSA (Sigma) for two hours in room temperature. Transplantation was performed with tungsten needle into the posterior PSM of decorionated embryos at the two-somite stage.

SU5402 (Calbiochem) treatment was performed with manually dechorionated embryos at the two-somite stage. SU5402 of 10 mg/ml in DMSO was used as a stock solution and diluted before use. Embryos were soaked for 8 minutes in the medium containing SU5402 at a concentration of 0.2 mg/ml (2% DMSO), followed by intense wash.

Detection of apoptosis

Apoptosis in zebrafish whole-mount was detected according to a protocol given by the manufacturer with some modifications (Dead End^{TM} Colorimetric Apoptosis Detection System; Promega) (Gacrieli et al., 1992). After fixation overnight in 4% paraformaldehyde (PFA) in PBS, embryos were transferred in methanol and then rehydrated in PBST (PBS/0.1% Tween 20). Subsequently, embryos were digested in 5 μg/ml proteinase K in PBS for 5 minutes and postfixed for 20 minutes in 4% PFA in PBS. The embryos were then immersed in acetone for 7 minutes at –20°C and incubated in the equilibration buffer (provided in the kit) for 10 minutes at the room temperature (RT). After incubation 3 hours at 37°C in working strength terminal deoxynucleotidyl transferase (TdT) enzyme, the DNA end-labelling reaction using biotinylated dUTP was stopped by washing in 2×saline sodium citrate (SSC) and PBST. Biotin was detected by horseradish-peroxidase-labelled streptavidin with diaminobenzidine (DAB).

Laser-assisted uncaging

Labelling PSM cells using caged fluorescein-dextran was performed mainly following that described by Gristsman et al. (Gristsman et al., 2000). 2% solution of dextran, DMNB-caged fluorescein and biotin (D-7146, Molecular probe) was injected into one- to two-cell-stage embryos. The embryos were left to develop under dark condition until use. Uncaging was performed with a few second pulse of 365 nm pulsed nitrogen laser (Laser Science) focused through a 40× dry objective of Zeiss Axioskop2 microscope. To ensure labeling of PSM cells at different levels of depth, the focus of the objective was changed at several times. Fluorescent and Nomarski images were sequentially acquired using chilled CCD (Hamamatsu Photonics), adjusted individually and overlaid.

RESULTS

Activation of Fgf/MAPK pathway in the posterior PSM

We have examined the spatial activation of Fgf/MAPK cascade by using a specific antibody against doubly phosphorylated ERK (dpERK), which is one of the downstream targets of activated receptor tyrosine kinases (RTK), including Fgfrs (Gotoh and Nishida, 1996; Christen and Slack, 1999; Cobb and Goldsmith, 1995). Strong activation of ERK is detected in the PSM as well as in the telencephalon and midbrain/hindbrain boundary (Fig. 1A). Histological sections of stained embryos at the three-somite stage reveal that the level of ERK activation is highest in the tailbud and maintained high over the intermediate PSM. The anterior PSM is devoid of dpERK, spanning over about a four- to five-somite wide domain posterior to the last formed somite (Fig. 1B). The expression pattern of zebrafish *fgf8* closely resembles that of dpERK (Fig. 1D,G,J,M) and, at least, one of the Fgfrs, *FGFR1*, is expressed in the entire PSM (Fig. 1N) (Sawada et al., 2000). The ERK activation and *fgf8* expression is also detected in newly formed somites (arrowheads in Fig. 1D,G,J,M).

Although ERK activation is triggered by downstream targets of various RTKs (Cobb and Goldsmith, 1995), the activation at segmentation stage is mainly attributable to an Fgf signal (see Discussion). When developing embryos were soaked for 8 minutes in medium containing 0.2 mg/ml of SU5402, a kinase inhibitor specific to perhaps all types of Fgfrs (Mohammadi et al., 1997), the dpERK staining is instantly and greatly reduced (Fig. 1C). After brief treatment, the level of ERK activation is gradually recovered within 3 hours (Fig. 1O).

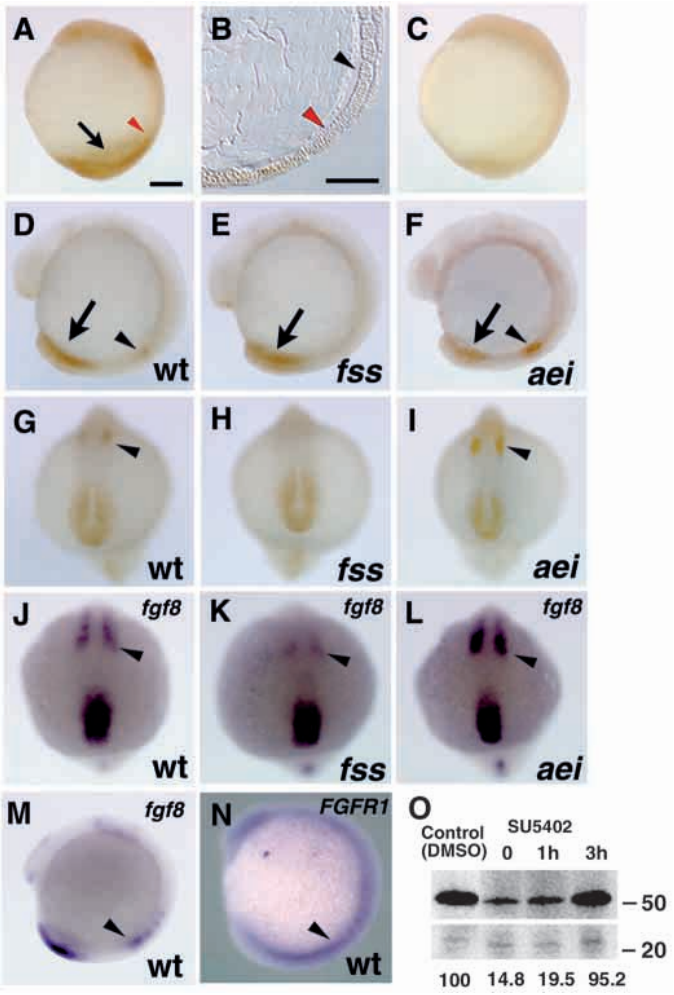

Fig. 1. Fgf/MAPK signalling in the presomitic mesoderm (PSM). Lateral views with anterior towards the top (A-F,M,N) and dorsal views with anterior towards the top (G-L) are shown. Black arrows indicate ERK activation domain in the PSM. (A) Immunostaining of a two-somite embryo with an antibody against an activated (di-phosphorylated) form of ERK (MAPK). The activation is detected in the anterior telencephalon, midbrain/hindbrain boundary and the PSM (arrow). (B) A sagittal section, taken from a three-somite embryos, shows that the anterior PSM, approximately four- to five-somite wide, is devoid of staining. Black arrowhead in B indicates the last formed somite boundary; red arrowheads in A,B roughly indicate the anterior border of the positive staining in PSM. (C) The immunostaining (at the three-somite stage) is greatly reduced after 8 minutes exposure to SU5402. (D-I) The activation pattern of ERK at the 10-somite stage in wild-type (D,G), *fused somites* (*fss*; E,H) and *after eight/deltaD* (*aei*; F,I) embryos. Black arrowheads indicate the activation in newly formed somites. Because *fss* embryos show no segmentation, they were fixed when their siblings reached the 10-somite stage. (J-M) *fgf8* expression at the 10-somite stage in wild-type (J,M), *fss* (K) and *aei* (L) embryos. Black arrowheads indicate the expression in newly formed somites. (N) *FGFR1* expression at the 10-somite stage in wild type. Broad expression in the PSM and anterior restricted expression in segmented somites are observed. The black arrowhead indicates the expression in newly formed somite. (O) In a western blot, the antibody recognizes a major band about 50 kDa, whose level is sensitive to SU5402. The intensity of each band was normalized by use of a SU5402-insensitive minor band (about 25 kDa, shown in the lower panel). The relative intensity is shown at the bottom of each lane. Scale bars: 100 μm (bar in A is applicable to A,C-N).

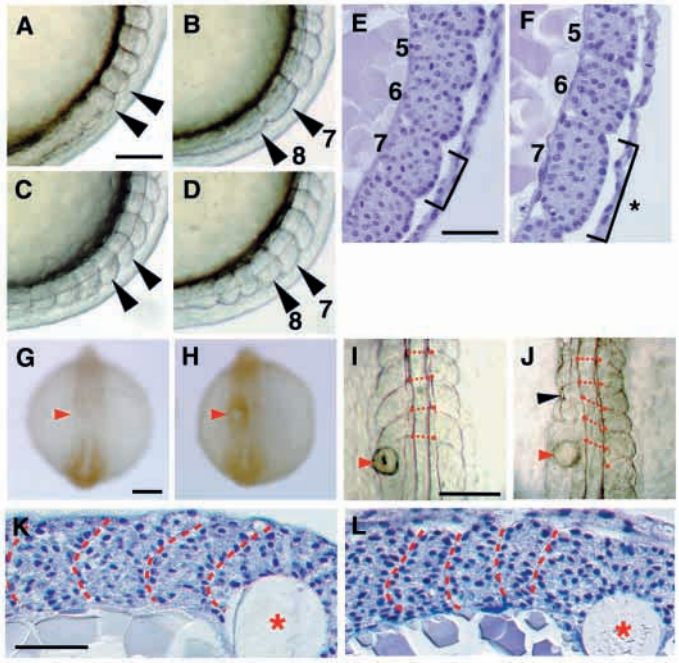

Fig. 2. Manipulation of an Fgf signal alters somite size. (A-F) The effect of SU5402 treatment on somitogenesis. Lateral views of live embryos at the seven-somite (A,B) and at the 10-somite (C,D) are shown. The somite number is indicated by numbers near the somites. The embryos were incubated in control (A,C) or SU5402-containing medium (B,D) for 8 minutes at the two-somite stage, followed by intense washing. Larger somites (arrowheads in B,D) are observed at the level of seventh and eighth somites, as compaired with those of a control embryo (arrowheads in A,C). (E,F) Sagittal sections from control (E) and treated (F) embryos confirm the formation of large somites. Note that a large somite (asterisk in F) contains more somitic cells that exhibit no cellular abnormality. (G-J) Transplantation of Fgf-soaked beads. Dorsal views are shown with anterior towards the top. The beads soaked in the medium containing Fgf8b or BSA (control) were transplanted on the left side of the tailbud region at the two-somite stage and fixed after various time periods. Red arrowheads indicate the location of the beads in the paraxial mesoderm. (G,H) Ectopic ERK activation is induced by Fgf-soaked bead (H) but not by a control bead (G). (I,J) The control bead does not affect somitogenesis (I). By contrast (J), the segment borders are anteriorly displaced and a small somite (black arrowhead) is formed anterior to the Fgf bead. Red circles along both sides of the notochord indicate the positions of the segment border, and the circles corresponding to each segment are connected with a broken line. (K,L) Sagittal sections (anterior to the left) of the segmented mesoderm from the embryos transplanted with BSA- (K) or Fgf8b-soaked (L) beads (red asterisks). The segment borders are indicated by broken lines. Regular spaced somites are seen anterior to the BSA beads, while the boundary formation is disturbed and smaller somites are formed anterior to the Fgf8 bead. Scale bars: 100 μm in A,G,I; 50 μm in E,K. Bar in A applies to A-D; bar in E applies to E,F; bar in G applies to G,H; bar in I aplies to I,J; bar in K applies to K,L.

Transient manipulation of Fgf signalling alters somite size

To explore the role of Fgf/MAPK signal in the PSM, we manipulated the level of Fgf signalling and observed the consequences upon somite formation. Treatment at the two-somite stage with SU5402 for 8 minutes resulted in the formation of abnormally large somites after a period of four to

five rounds of normal somite formation (Fig. 2A,B) (about 10 to 12 cells wide instead of six to eight cells wide in normal somites; the axial length of the seventh somite was 72 μm±3.8, *n*=10 after SU5402 treatment but 49 μm±5.7 for control treatment). Increase in somite size (Fig. 2E,F), however, is limited to one or two consecutive somites, and, thereafter, normal somite formation resumes, although the somites just posterior to the large ones are sometimes smaller in size (Fig. 2C,D). Histological sections confirm that the large somites do not show any cellular abnormalities such as apoptosis or increase in cell volume, but simply contain a larger number of somitic cells (Fig. 2E,F), except for a restricted cell death occasionally observed in the tailbud at later stages. Furthermore, the segmental expression of *mesp* and *papc*, markers for the anterior part of prospective and/or segmented somites, confirms that anteroposterior specification within large somites normally takes place (Fig. 3G-I).

We then performed a reverse experiment by transplanting

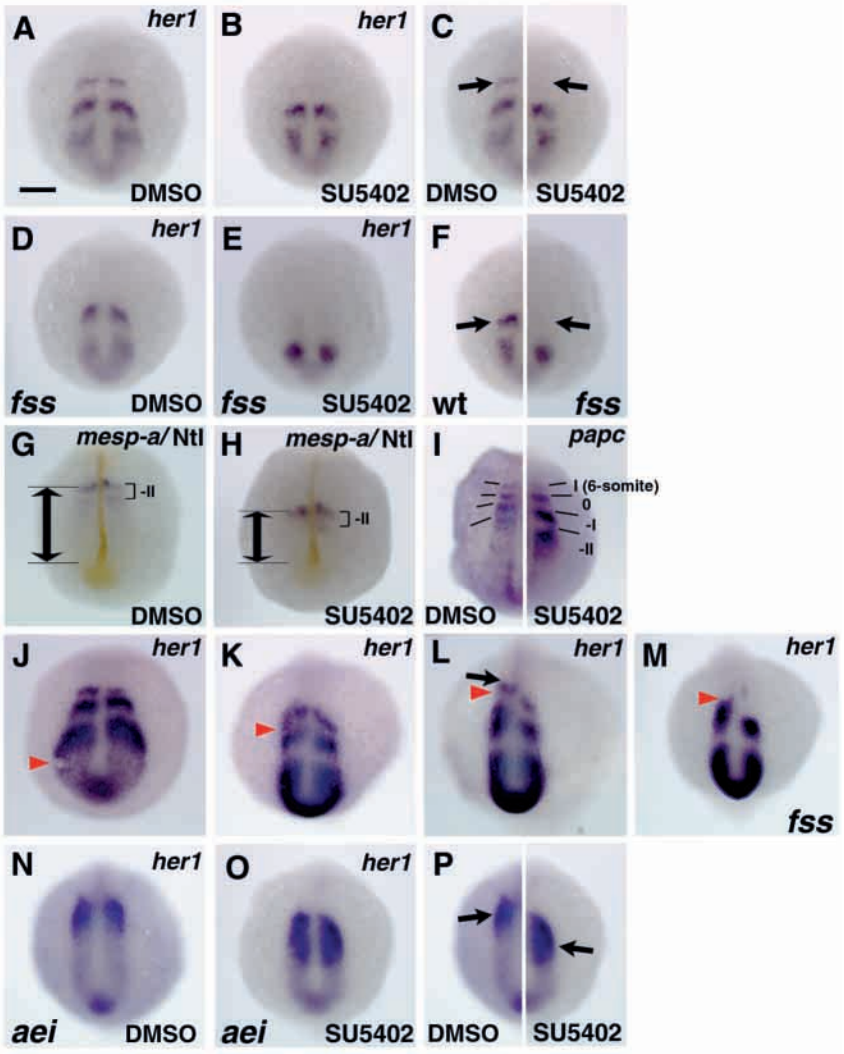

Fig. 3. Gene expression analyses. Dorsal views are shown with anterior towards the top. (A-C) *her1* expression in control (A) and SU5402-treated (B) embryos. The embryos were treated with SU5402 for 8 minutes at the two-somite stage and fixed at the six-somite stage when the prospective large somites are being specified. For comparison, the left half of the control embryo shown in A and the right half of the treated embryo shown in B are shown as a composite (C). In treated embryos, the anterior *her1* stripe is missing. Arrows indicate the level of the anterior *her1* stripe in a control embryo. (D-F) *her1* expression in *fused somite* (*fss*) mutants after treated with control (D) or SU5402 (E) medium. A composite (F), the left half of SU5402-treated wild-type embryo shown in B and the right half of SU5402-treated *fss* embryo in E, shows that the *her1* stripe in the intermediate PSM is not maintained in $fss^{-/-}$ background after SU5402 treatment. The arrows in F indicate the level of the intermediate (anteriormost in this case) *her1* stripe in the embryo shown in B. As *fss* embryos show no segmentation, the embryos were treated with SU5402 for 8 minutes when their siblings reached the two-somite stage, and they were fixed when their siblings reached the six-somite stage. (G,H) *mesp-a* expression at the six-somite stage in control (G) and SU5402-treated (H) embryos. The embryos were treated with SU5402 for 8 minutes at the two-somite stage, fixed at the six-somite stage and followed by in situ hybridization with *mesp-a* (blue) probe. To make clear the relationship between the *mesp-a* stripe and the tailbud (indicated by double-headed arrows), the embryos were also stained with the antibody against No tail (Ntl). The notochord and the tailbud is positive for the antibody (yellow). The anterior *mesp-a* expression domain, which normally demarcates the somite primordium at the position of –II (G) (Durbin et al., 2000; Sawada et al., 2000), posteriorly shifts to the intermediate PSM (H) after treatment of SU5402. (I) A composite picture of *papc* expression at the six-somite stage in control (left) and SU5402-treated (right) embryos. *papc* is expressed in four bilateral pairs of stripes in the paraxial mesoderm during the segmentation period (Yamamoto et al., 1998). The first stripe is located in the anterior border of the newest somite formed (I) and the second in the forming somite (0). The two posterior, stronger and broader stripes seem to be located in successive somite primordia (-I and -II). In treated embryos, the positions of the posterior two stripes are posteriorly displaced when compared with control embryos with a wider interval between them. (J-M) *her1* expression in the PSM exposed to exogenous Fgfs. The embryos were transplanted with Fgf beads at the two-somite stage, and fixed at the two-somite (J), five-somite (K) and eight-somite (L,M) stages. Red arrowheads indicate the location of the beads in the PSM. The intermediate *her1* stripe is anteriorly expanded around the Fgf bead with the posterior border unchanged (L); the anterior *her1* stripe is located in more anterior region than on the control side (arrow in L). In *fss* embryo, the transplanted Fgf-bead exerts the same effect on the intermediate *her1* stripe (M; compare with L). Note that the anterior *her1* stripes are always missing in *fss* embryos on both sides of the PSM. (N-P) *her1* expression in *after eight* (*aei*) mutant after treatment with control (N) or SU5402 (O) medium. A composite (P) shows that the anterior *her1* expression shifts posteriorly to the intermediate PSM after treatment with SU5402. The arrows in P indicate the level of the anteriormost *her1* expression in control and treated *aei* embryos. In *aei* mutants, the first eight to ten somites are normally formed and, thereafter, defects in boundary formation are evident. Thus, the embryos were treated with SU5402 at the four-somite stage, and fixed at the eight-somite stage (later stages than other experiments). The genotyping of the embryos was carried out using PCR (Holley et al., 2000). Scale bar: 100 μm.

Fgf8-soaked beads. Transplanted Fgf8 but not control beads induced ectopic activation of ERK (Fig. 2G,H). The resulting phenotype is opposite to that obtained with the treatment of SU5402; on the transplanted side, the segment borders are anteriorly displaced and smaller somites are formed in the region anterior to the Fgf bead (Fig. 2I-L). Although the severity of the phenotype varied a great deal, statistical data show that the posterior border of the somite just anterior to a Fgf8b bead shifts by a distance of more than half a somite length (36±19 μm (*n*=10)) to that of the corresponding somite on the control side. Thus, the somite size can be controlled by manipulation of an Fgf signal in the PSM.

Alterations in somite size are caused by an altered pace of wavefront progression

According to the 'clock-and-wavefront' (Cooke and Zeeman, 1976; Dale and Pourquié, 2000) model, the somite size is a function of the frequency of the segmentation clock and of the velocity of the maturation wavefront. Increase in somite size could therefore be achieved either by slowing down the oscillation or by accelerating the wavefront progression. To test this, we examined the cyclic expression of *her1*, a gene encoding a *hairy*-related bHLH transcription factor, in treated embryos. As shown in Fig. 3A, *her1* expression usually appears as three stripes in the PSM (referred to as posterior, intermediate and anterior stripes) (Fig. 4A). A new wave of *her1* expression appears in the tailbud every 30 minutes (the duration of one-somite formation in zebrafish), becomes narrower as it moves rostrally and finally stabilizes at the future segmentation point in the anterior PSM before decaying (Sawada et al., 2000; Holley et al., 2000). The expression pattern of *her1* was examined at the six-somite when the prospective large somites were forming in the PSM after treatment at the two-somite stage. Comparison with control embryos reveals that the *her1* stripe in the anterior PSM is always undetectable with the posterior two stripes intact (Fig. 3A-C), indicating that, after SU5402 treatment, the *her1* cyclic expression prematurely terminates in the intermediate PSM, instead of the anterior PSM (the length from tailbud to the anterior border of the expression stripe (L)=566±23.3 μm for control (*n*=10) and 446±28.8 μm for SU5402 treated embryos (*n*=10)). The operation of the oscillator seems to be unaffected because a variety of posterior expression patterns are seen in treated embryos fixed at the same stage, implying a cyclic expression (data not shown). More importantly, somites are regularly specified (compare Fig. 2B,D with 2A,C), despite size difference, and an interval between intermediate and posterior *her1* stripes is unchanged in treated embryos at any stage examined (Fig. 3B,C), indicating a normal pace of oscillation.

There are at least two explanations for premature termination of *her1*: (1) the anterior PSM is unable to maintain the anterior *her1* expression, owing to defects in maturation processes, as in the case of *fused somites* (*fss*) mutants (van Eeden et al., 1996; van Eeden et al., 1998); (2) the position of the maturation wavefront that arrests the cyclic wave shifts posteriorly due to an accelerated maturation of the PSM. Recent analyses in zebrafish mutants have shown that *her1* expression has two genetically separable domains (Holley et al., 2000; Jiang et al., 2000; van Eeden et al., 1998): cyclic *her1* expression requires Notch/Delta signalling, and it becomes stabilized in the anterior PSM in a *fss*-dependent manner because only the anterior *her1* stripe is affected and missing in *fss* embryos (Fig. 3D). Although the *her1* expression pattern is similar in SU5402-treated embryos and *fss* embryos (compare Fig. 3B with 3D), their somitogenesis phenotypes are totally different (large somites versus no segmentation), indicating that the failure in maintaining the anterior *her1* stripe in SU5402-treated embryos is not due to somite maturation defects. When treated with SU5402, *fss* embryos become

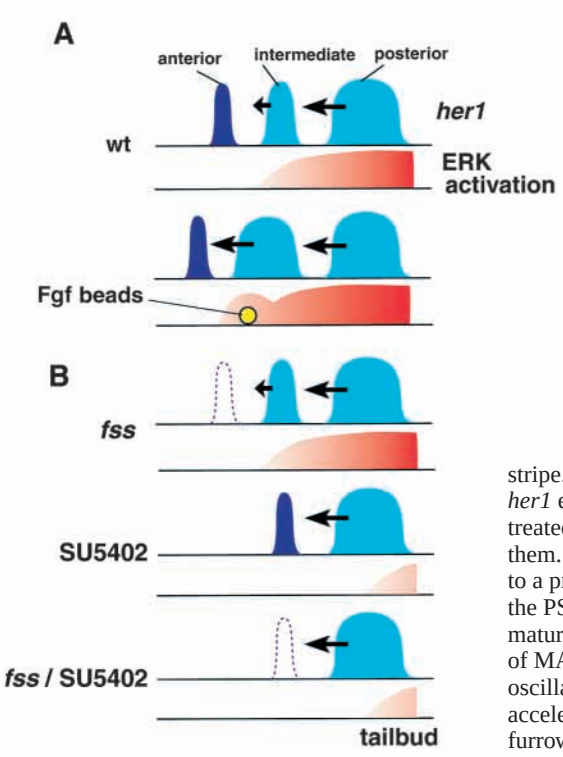

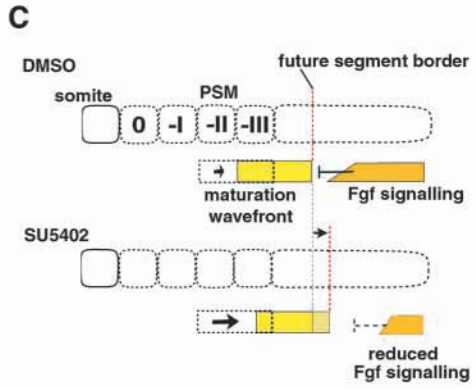

Fig. 4. Models of how Fgf/MAPK signalling is involved in somite boundary formation. (A) An exogenous Fgf signal in the anterior PSM maintains the PSM in an immature status for a longer period. This anteriorized the position at which the domain transition of the *her1* cyclic expression, from the cycling (in light blue) to the stabilized (in dark blue), takes place. This results in an anteriorly expanded intermediate *her1* stripe. (B) In *fss* embryos, anterior *her1* stripe is missing, owing to maturation defects. The *her1* expression pattern in *fss* embryos is apparently similar to that in wild-type embryos treated with SU5402. However, SU5402 treatment of *fss* embryos discriminates between them. In wild-type embryos treated with SU5402, the anterior *her1* stripe disappears owing to a premature domain transition of *her1* expression induced by accelerated maturation of the PSM. (C) An Fgf signal activated in the intermediate and posterior PSM antagonizes maturation of PSM cells. In the maturation wavefront, the anterior PSM, which is devoid of MAPK activation, becomes competent to initiate furrow formation in response to the oscillator. When an Fgf signal is transiently compromised by SU5402, the maturation is accelerated and the wavefront is posteriorly expanded, which leads to a posterior shift in furrow formation. The presumptive somites are indicated by Roman numerals.

unable to maintain the intermediate *her1* stripe in addition to the anterior one, and, consequently, *her1* is expressed only in the tailbud (Fig. 3E,F) (L=477±27.1 μm for control *fss* (*n*=10) and 358±19.9 μm for SU5402-treated *fss* embryos (*n*=10)). Thus, *fss*-dependent domain transition of *her1* expression, which normally takes place in the corresponding anterior PSM region, shifts to the corresponding intermediate PSM region when Fgf signalling is compromised (Fig. 4B). Morphologically, this premature transition is accompanied by a posterior shift in furrow formation as indicated by other segmentation genes. For example, the expression domain of *mesp*, a bHLH transcription factor crucial for segmentation initiation (Sawada et al., 2000; Saga et al., 1997; Durbin et al., 2000), posteriorly shifts after treatment (Fig. 3G,H). Similarly, the posterior two stripes of *paraxial protochadherin* (*papc*) (Yamamoto et al., 1998), which correspond to the region where large somites are being specified, are posteriorly displaced with a larger interval between them (-I, -II in Fig. 3I), while the anterior two stripes, which demarcate the anterior borders of the newly formed (I) and forming (0) somites, remain unchanged (Fig. 3I). We conclude from all these results that large somites are produced in SU5402-treated embryos by a transient posterior shift in furrow formation, owing to acceleration of maturation or wavefront progression in the PSM (Fig. 4C).

We further examined the effect of exogenous Fgfs on *her1* expression. Embryos were implanted with Fgf-soaked beads into the tailbud at the two-somite stage, and were fixed at various times after implantation. The bead does not significantly affect the pattern of *her1* expression when located in the posterior to intermediate PSM (Fig. 3J,K). However, as the bead passes the intermediate to anterior PSM, the anterior boundary of the intermediate *her1* stripe is anteriorly displaced when compared with that on the control side (Fig. 3L). In another words, the anterior part of the intermediate stripe does not reduce the slowing down rate and moves more anteriorly, resulting in an anteriorly broaden stripe. Transplantation of Fgf beads into *fss* embryos confirms that the affected *her1* stripe is *fss* independent (Fig. 3M). Eventually, on the transplanted side, the *her1* expression reaches more anteriorly than it does on the control side (Fig. 3L), which may cause an anterior shift in furrow formation, explaining the formation of smaller somites anterior to the transplanted beads. Taken together, the prolonged activation of Fgf/MAPK signalling delays maturation of PSM cells, and anteriorizes the domain transition of *her1* expression (Fig. 4B), resulting in an anterior shift in furrow formation.

Fgf/MAPK signalling functions independently of the Notch or Fss pathway

To determine whether the Fgf-mediated positioning of PSM maturation is influenced by Notch/Delta pathway, we performed SU5402 treatment in *after eight* (*aei*) mutants, in which *deltaD* gene is defective (Holley et al., 2000). In *aei* embryos, the synchronized wave of *her1* is lost (Jiang et al., 2000), while the mature anterior PSM expresses *her1*, *deltaC* and *mesp* (Fig. 3N) (Holley et al., 2000; Jiang et al., 2000; Sawada et al., 2000). As in wild-type (Fig. 3A-C) and *fss* (Fig. 3D,E) embryos, SU5402 treatment shifts the expression domains of *her1* (Fig. 3N-P) to the intermediate region in *aei* mutants (L=520±22.6 μm for control *aei* (*n*=10) and 441±27.3 μm for SU5402-treated *aei* (*n*=10)). Furthermore, the activation pattern of ERK and the expression pattern of *fgf8* in the PSM do not significantly change in *fss* and *aei* mutants (Fig. 1D-F). Their patterns in the segmented somites, however, varies in mutant embryos; nearly undetectable in *fss* (Fig. 1E,H,K) but tending to increase in *aei* mutants (arrowheads in Fig. 1F,I,L). Thus, the action of Fgf signalling in the PSM is likely to be independent of Notch/Delta and Fss pathways.

Manipulation of Fgf/MAPK signalling does not affect proliferation or behaviour of PSM cells

Finally, we tested whether the manipulation of Fgf/MAPK signalling affects cell death, cell proliferation and cell migration in the PSM. The numbers of apoptotic and mitotic cells were counted in histological sections of treated embryos by a modified TUNEL method (Gavrieli et al., 1992) and immunohistochemical staining with anti-phosphorylated histone H3 that recognizes cells in M phase (Saka and Smith, 2001). As summarized in Table 1, no significant difference was observed in cell death and proliferation in the PSM after manipulation of an Fgf signal (Fig. 5A-D). Cell behaviour in the PSM was examined by a photoactivation technique of caged substances (Gritsman et al., 2000). One- to two-cell embryos were injected with caged fluorescein-dextran dye and left to develop to the two-somite stage, when Fgf8-soaked beads were transplanted into the tailbud region. We then labelled, by laser-assisted uncaging, a group of PSM cells located anterior to the beads, as well as cells at the same axial level on the control side (Fig. 5E). The positions of those labelled cells were examined after 5 hours' incubation (12-somite stage). As shown in Fig. 5F, although the somite boundaries are anteriorly displaced on the transplanted side, the axial position of labelled cells does not significantly change between the control and transplanted sides, indicating that no specific cell migration is induced by exogenous Fgfs.

DISCUSSION

In the present study, we have analysed the function of Fgf/MAPK signalling in zebrafish somitogenesis, focusing on

Table 1. Effects of Fgf manipulations on cell death and proliferation in the PSM

	Inhibitor treatment		Bead transplantation	
Type of treatment	SU5402 (*n*)	DMSO (*n*)	Fgf8b (*n*)	BSA (*n*)
Proportion of apoptotic cells	2.6±2.0% (10)	3.2±2.2% (10)	1.5±0.77% (5)	2.6±1.4% (5)
Proportion of cells in M phase	3.3±1.6% (10)	3.2±0.9% (12)	2.7±1.1% (6)	3.0±1.8% (6)

The mean±s.d. is presented.
n, the number of samples counted.
In inhibitor treatment, about 200 cells in the intermediate to anterior PSM were counted in each sample.
In bead transplantation, about 200 cells located anterior to the bead were counted in each sample.

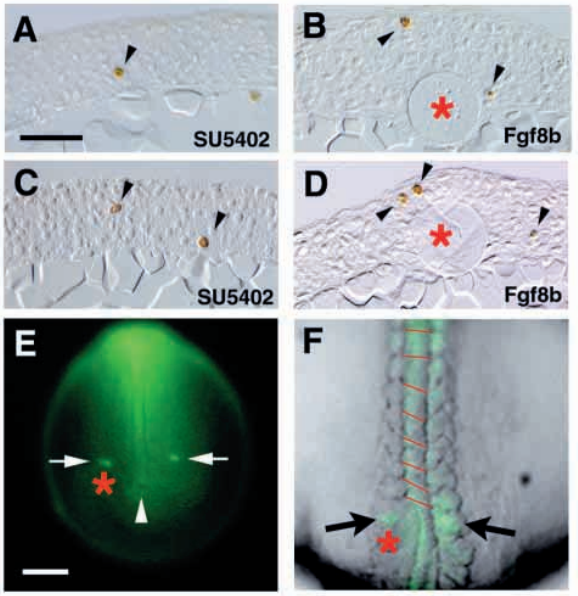

Fig. 5. The effects of Fgf manipulation on cell death, proliferation and migration in the PSM. (A,B) Sagittal sections (anterior towards the left) showing apoptotic cells (brown, arrowheads) in the PSM after SU5402 treatment (A) and Fgf8b-bead (asterisk) transplantation control (B). (C,D) Sagittal sections (anterior to the left) showing cells in M phase (brown, arrowheads) in the PSM after SU5402 treatment (C) and in an Fgf8b-bead (asterisk) transplantation control (D). (E,F) Cell lineage analysis in the PSM. Fgf8b-soaked bead (asterisks) was transplanted in the tailbud of two-somite stage embryos injected with cased fluorescein. A group of PSM cells at the same axial level of both transplanted and control sides were then fluorescently labelled by laser-assisted uncaging (E). A white arrowhead indicates the tailbud. The relative position of labelled cells (arrows) is still maintained when examined at the 12-somite stage after 5 hours' incubation (F), although the points of segment furrow formation are anteriorly displaced on the transplanted side. Each segment border of the same numbered somites is connected by a red line. Scale bars: in A, 50 μm for A-D; in E, 100 μm for E,F.

the events in the PSM. The staining data show that ERK, a vertebrate MAPK, is activated in the posterior two thirds of the PSM. As in *Xenopus* embryos (Christen and Slack, 1999), ERK activation at segmentation stages mostly depends on Fgf signalling because the activation is greatly suppressed after injection of RNAs encoding dominant-negative forms of Fgf-R (Shinya et al., 2001) and treatment of SU5402. Furthermore, ectopic activation of ERK was induced around the transplanted Fgf8 beads, while no such activation was detected around BSA-soaked bead (Fig. 2G,H). The temporal and spatial pattern of ERK activation correlates well with that of *fgf8* expression at segmentation stages, suggesting that Fgf8 is a major activator of MAPK pathway in zebrafish. However, in zebrafish *acerebellar* (*ace*) mutant in which no functional Fgf8 is produced (Reifers et al., 1998), substantial amount of ERK activation persists (about 50% of wild-type activation) (Shinya et al., 2001) and no clear posterior shift in somite boundary formation is observed (Reifers et al., 1998). Therefore, some other Fgfs must be responsible for ERK activation and involved in zebrafish somite maturation.

Modulating Fgf signalling resulted in alterations in somite size. Detailed analyses of gene expressions in manipulated wild-type and mutant embryos revealed a novel function of Fgf/MAPK signalling in the PSM, the maintenance of cells in an immature state that allows the *her1* wave to sweep through the PSM. Suppression of Fgf signalling posteriorizes the domain shift of *her1* expression, as well as the expression of other segmentation genes such as *mesp* and *papc*. This leads to a posterior shift in segment border formation and larger somites. These results are complementary to those obtained with transplantation of Fgf beads, strengthening the idea that an Fgf signal determines the position of segment border formation by negatively regulating the maturation of the PSM. As Fgf signal is known to have profound effects on many developmental processes such as cell growth and maintenance of progenitor cells (Szebenyi and Fallon 1999; Mathis et al., 2001), it is possible that manipulation of an Fgf signal locally changes the cell number in the PSM by regulating cell proliferation and/or cell migration within the mesoderm (axial, paraxial and lateral plate mesoderm). This could cause alterations in somite size. However, no such effect was observed in manipulated PSM, indicating that an Fgf signal in the PSM simply regulates the maturation status of cells without affecting cell proliferation or migration.

Our data are largely consistent with the 'clock-and-wavefront' model in which a cyclic wave operates in conjunction with a maturation wavefront that gradually moves posteriorly, resulting in arrest of the cyclic wave and initiation of segment furrow formation (Cooke and Zeeman, 1976; Dale and Pourquié, 2000). Fgf/MAPK signalling negatively regulates the wavefront activity and restricts it to the anterior PSM that is devoid of MAPK activation (Fig. 4C). In zebrafish, the essential components of a conserved somite-making mechanism, the segmentation clock and wavefront, were shown to be Notch- and Fss-dependent, respectively. Zebrafish *aei/deltaD* mutation desychronizes the oscillation wave (Jiang et al., 2000), while, in the absence of Fss, the anterior PSM fails to acquire the wavefront activity (Holley et al., 2000). How could Fgf/MAPK signal interact with these components? In fact, it has been reported that the Ras/MAPK pathway interacts with the Notch pathway in *C. elegans* vulval development (Sundaram and Han, 1996) and malignant transformation of cultured cells (Fitzgerald et al., 2000). However, we failed to show any interaction between Fgf/MAPK and Notch or Fss pathways: modulating Fgf signalling exerts identical effects on wild-type and *aei/DeltaD* or *fss* mutants in terms of gene expression. Furthermore, the patterns of ERK activation and *fgf8* expression in the PSM is not affected by *aei/DeltaD* and *fss* mutations. Thus, we conclude that the activation and action of Fgf/MAPK signalling in the PSM are not mediated by Notch or Fss pathway.

The fact that four to five somites are normally formed after SU5402 treatment indicates that the positioning of furrow formation is already specified or Fgf insensitive at least at the position -IV to -V in the PSM (Fig. 4C). The result also indicates that ERK activation in segmented somites (arrowheads in Fig. 1D,G,J,M) is not involved in segment border formation. Interestingly, the Fgf-sensitive region corresponds approximately to the heat-shock sensitive zone in zebrafish; that is, the initial defects in the segmental pattern of somite boundaries are observed five somites caudal to the forming somite at the time of heat shock (Roy et al., 1999). Our data suggest that position -IV to -V represents a position at which the level of Fgf/MAPK activation drops below a

threshold, rendering the cells competent to maturation signals (Fig. 1A,B). In support of this, transplanted Fgf8 beads exert their effects only when they are located in the Fgf-negative anterior PSM (Fig. 3K,L). Importantly, the relative position of MAPK activation domain to the newly formed somite is kept constant in the PSM as the embryos extend. These observations are consistent with the idea that the level of Fgf/MAPK activation serves as a positional cue within the PSM. Recently, Dubrulle et al. (Dubrulle et al., 2001) have demonstrated that Fgf signalling controls somite boundary position in chick embryos, indicating conserved mechanisms in somite boundary determination among vertebrates. The existence of positional information along the anteroposterior axis in the PSM has been proposed by the 'clock-and-wavefront' model (Cooke and Zeeman, 1976; Dale and Pourquié, 2000), and the present study is the first to provide evidence for the molecular identity of, at least, one positional cue that governs the positions of segment border formation, and thereby the size of somites.

We thank Dr Steve Wilson (Kings College London) and Dr Yumiko Saga (National Institute of Genetics) for discussion and critical reading of the manuscript. We also thank Dr Makoto Furutani-Seiki (Kondoh Differentiation Project, ERATO, JST) for kindly providing us *fss* mutants and Dr Kyo Yamasu (Saitama University) for zebrafish FGFR1 probe. This work was supported in part by Bio-Design Project (BDV-01-IV-1-7) and Pioneering Research Project in Biotechnology from the Ministry of Agriculture, Forestry and Fisheries of Japan, and by organized research combination and grants-in-aids from the Ministry of Education, Culture, Sports, Science and Technology of Japan. A. S. is supported by the Research Fellowships of the Japan Society for the Promotion of Science for Young Scientists.

REFERENCES

Aulehla, A. and Johnson, R. L. (1999). Dynamic expression of *lunatic fringe* suggests a link between notch signaling and an autonomous cellular oscillator driving somite segmentation. *Dev. Biol.* **207**, 49-61.

Christen, B. and Slack, J. M. (1999). Spatial response to fibroblast growth factor signalling in *Xenopus* embryos. *Development* **126**, 119-125.

Cobb, M. H. and Goldsmith, E. J. (1995). How MAP kinases are regulated. *J. Biol. Chem.* **270**, 14843-14846.

Cooke, J. and Zeeman, E. C. (1976). A clock and wavefront model for control of the number of repeated structures during animal morphogenesis. *J. Theor. Biol.* **58**, 455-476.

Dale, K. J. and Pourquié, O. (2000). A clock-work somite. *BioEssays* **22**, 72-83.

Dubrulle, J., McGrew, M. J. and Pourquie, O. (2001). FGF signaling controls somite boundary position and regulates segmentation clock control of spatiotemporal Hox gene activation. *Cell* **106**, 219-232.

Durbin, L., Sordino, P., Barrios, A., Gering, M., Thisse, C., Thisse, B., Brennan, C., Green, A., Wilson, S. and Holder, N. (2000). Anteroposterior patterning is required within segments for somite boundary formation in developing zebrafish. *Development* **127**, 1703-1713.

Fitzgerald, K., Harrington, A. and Leder, P. (2000). Ras pathway signals are required for notch-mediated oncogenesis. *Oncogene* **19**, 4191-4198.

Forsberg, H., Crozet, F. and Brown, N. A. (1998). Waves of mouse *Lunatic fringe* expression, in four-hour cycles at two-hour intervals, precede somite boundary formation. *Curr. Biol.* **8**, 1027-1030.

Gavrieli, Y., Sherman, Y. and Ben-Sasson, S. A. (1992). Identification of programmed cell death in situ via specific labeling of nuclear DNA fragmentation. *J. Cell Biol.* **119**, 493-501.

Gotoh, Y. and Nishida, E. (1996). Signals for mesoderm induction. Roles of fibroblast growth factor (FGF)/mitogen-activated protein kinase (MAPK) pathway. *Biochim. Biophys. Acta* **1288**, F1-F7.

Gritsman, K., Talbot, W. S. and Schier, A. F. (2000). Nodal signaling patterns the organizer. *Development* **127**, 921-932.

Holley, S. A., Geisler, R. and Nusslein-Volhard, C. (2000). Control of *her1* expression during zebrafish somitogenesis by a delta- dependent oscillator and an independent wave-front activity. *Genes Dev.* **14**, 1678-1690.

Jiang, Y. J., Aerne, B. L., Smithers, L., Haddon, C., Ish-Horowicz, D. and Lewis, J. (2000). Notch signalling and the synchronization of the somite segmentation clock. *Nature* **408**, 475-479.

Jiang, Y. J., Smithers, L. and Lewis, J. (1998). Vertebrate segmentation: the clock is linked to Notch signalling. *Curr. Biol.* **8**, R868-R871.

Jouve, C., Palmeirim, I., Henrique, D., Beckers, J., Gossler, A., Ish-Horowicz, D. and Pourquié, O. (2000). Notch signalling is required for cyclic expression of the *hairy*-like gene HES1 in the presomitic mesoderm. *Development* **127**, 1421-1429.

Kimmel, C. B., Ballard, W. W., Kimmel, S. R., Ullmann, B. and Schilling, T. F. (1995). Stages of embryonic development of the zebrafish. *Dev. Dyn.* **203**, 253-310.

Mathis, L., Kulesa, P. M. and Fraser, S. E. (2001). FGF receptor signalling is required to maintain neural progenitors during Hensen's node progression. *Nat. Cell Biol.* **3**, 559-566.

McGrew, M. J., Dale, J. K., Fraboulet, S. and Pourquié, O. (1998). The *lunatic fringe* gene is a target of the molecular clock linked to somite segmentation in avian embryos. *Curr. Biol.* **8**, 979-982.

Mohammadi, M., McMahon, G., Sun, L., Tang, C., Hirth, P., Yeh, B. K., Hubbard, S. R. and Schlessinger, J. (1997). Structures of the tyrosine kinase domain of fibroblast growth factor receptor in complex with inhibitors. *Science* **276**, 955-960.

Nikaido, M., Tada, M., Saji, T. and Ueno, N. (1997). Conservation of BMP signaling in zebrafish mesoderm patterning. *Mech. Dev.* **61**, 75-88.

Palmeirim, I., Henrique, D., Ish-Horowicz, D. and Pourquié, O. (1997). Avian *hairy* gene expression identifies a molecular clock linked to vertebrate segmentation and somitogenesis. *Cell* **91**, 639-648.

Pourquié, O. (1999). Notch around the clock. *Curr. Opin. Genet. Dev.* **9**, 559-565.

Reifers, F., Bohli, H., Walsh, E. C., Crossley, P. H., Stainier, D. Y. and Brand, M. (1998). Fgf8 is mutated in zebrafish *acerebellar* (*ace*) mutants and is required for maintenance of midbrain-hindbrain boundary development and somitogenesis. *Development* **125**, 2381-2395.

Roy, M. N., Prince, V. E. and Ho, R. K. (1999). Heat shock produces periodic somitic disturbances in the zebrafish embryo. *Mech. Dev.* **85**, 27-34.

Saga, Y., Hata, N., Koseki, H. and Taketo, M. M. (1997). *Mesp2*: a novel mouse gene expressed in the presegmented mesoderm and essential for segmentation initiation. *Genes Dev.* **11**, 1827-1839.

Saka, Y. and Smith, J. C. (2001). Spatial and temporal patterns of cell division during early Xenopus embryogenesis. *Dev. Biol.* **229**, 307-318.

Sawada, A., Fritz, A., Jiang, Y., Yamamoto, A., Yamasu, K., Kuroiwa, A., Saga, Y. and Takeda, H. (2000). Zebrafish *Mesp* family genes, *mesp-a* and *mesp-b* are segmentally expressed in the presomitic mesoderm, and Mesp-b confers the anterior identity to the developing somites. *Development* **127**, 1691-1702.

Shinya, M., Koshida, S., Sawada, A., Kuroiwa, A. and Takeda, H. (2001). Fgf signalling through MAPK cascade is required for development of the subpallia/telencephalon in zebrafish embryos. *Development* **128**, 4153-4164.

Sun, X., Meyers, E. N., Lewandoski, M. and Martin, G. R. (1999). Targeted disruption of Fgf8 causes failure of cell migration in the gastrulating mouse embryo. *Genes Dev.* **13**, 1834-1846.

Sundaram, M. and Han, M. (1996). Control and integration of cell signaling pathways during C. elegans vulval development. *BioEssays* **18**, 473-480.

Szebenyi, G. and Fallon, J. F. (1999). Fibroblast growth factors as multifunctional signaling factors. *Int. Rev. Cytol.* **185**, 45-106.

van Eeden, F. J., Granato, M., Schach, U., Brand, M., Furutani-Seiki, M., Haffter, P., Hammerschmidt, M., Heisenberg, C. P., Jiang, Y. J., Kane, D. A. et al. (1996). Mutations affecting somite formation and patterning in the zebrafish, *Danio rerio*. *Development* **123**, 153-164.

van Eeden, F. J., Holley, S. A., Haffter, P. and Nusslein-Volhard, C. (1998). Zebrafish segmentation and pair-rule patterning. *Dev. Genet.* **23**, 65-76.

Yamaguchi, T. P., Conlon, R. A. and Rossant, J. (1992). Expression of the fibroblast growth factor receptor FGFR-1/flg during gastrulation and segmentation in the mouse embryo. *Dev. Biol.* **152**, 75-88.

Yamaguchi, T. P., Harpal, K., Henkemeyer, M. and Rossant, J. (1994). fgfr-1 is required for embryonic growth and mesodermal patterning during mouse gastrulation. *Genes Dev.* **8**, 3032-3044.

Yamamoto, A., Amacher, S. L., Kim, S. H., Geissert, D., Kimmel, C. B. and De Robertis, E. M. (1998). Zebrafish paraxial protocadherin is a downstream target of spadetail involved in morphogenesis of gastrula mesoderm. *Development* **125**, 3389-3397.